NeuroImage 274 (2023) 120141

Contents lists available at ScienceDirect

NeuroImage

journal homepage: www.elsevier.com/locate/neuroimage

Crossmodal plasticity following short-term monocular deprivation

Alessandra Federici [a,*], Giulio Bernardi [a], Irene Senna [b], Marta Fantoni [a], Marc O. Ernst [c], Emiliano Ricciardi [a], Davide Bottari [a]

[a] MoMiLab, IMT School for Advanced Studies Lucca, 55100 Lucca, Italy
[b] Department of Psychology, Liverpool Hope University, United Kingdom
[c] Applied Cognitive Psychology, Ulm University, 89081 Ulm, Germany

ARTICLE INFO

Keywords:
Neural plasticity
Multisensory
Crossomdal
Monocular deprivation
EEG
Neural oscillations

ABSTRACT

A brief period of monocular deprivation (MD) induces short-term plasticity of the adult visual system. Whether MD elicits neural changes beyond visual processing is yet unclear. Here, we assessed the specific impact of MD on neural correlates of multisensory processes. Neural oscillations associated with visual and audio-visual processing were measured for both the deprived and the non-deprived eye. Results revealed that MD changed neural activities associated with visual and multisensory processes in an eye-specific manner. Selectively for the deprived eye, alpha synchronization was reduced within the first 150 ms of visual processing. Conversely, gamma activity was enhanced in response to audio-visual events only for the non-deprived eye within 100–300 ms after stimulus onset. The analysis of gamma responses to unisensory auditory events revealed that MD elicited a crossmodal upweight for the non-deprived eye. Distributed source modeling suggested that the right parietal cortex played a major role in neural effects induced by MD. Finally, visual and audio-visual processing alterations emerged for the induced component of the neural oscillations, indicating a prominent role of feedback connectivity. Results reveal the causal impact of MD on both unisensory (visual and auditory) and multisensory (audio-visual) processes and, their frequency-specific profiles. These findings support a model in which MD increases excitability to visual events for the deprived eye and audio-visual and auditory input for the non-deprived eye.

1. Introduction

In recent years, evidence that basic visual functions retain plastic potential even in the adult brain has accumulated (Karmarkar and Dan, 2006; Spolidoro et al., 2009; Espinosa and Stryker, 2012; Hensch and Quinlan, 2018). Studies in adults employing psychophysics and neuroimaging methods showed that a brief period of monocular deprivation (MD) alters the ocular balance by strengthening visual processing of the deprived eye and weakening the non-deprived eye (see Lunghi et al., 2011 for the first evidence, see Castaldi et al., 2020 for a review). These functional changes reflect ocular dominance shifts in V1 in favor of the deprived eye (Lunghi et al., 2015a; Binda et al., 2018) and are supposedly driven by homeostatic plasticity (Lunghi et al., 2015b), a mechanism underpinning the cortical excitatory-inhibitory balance (Turrigiano, 2012).

Besides the effects on the visual system, MD also seem to alter multisensory processing. At the behavioral level, short-term MD was found to affect the interaction between sensory modalities (Lo Verde et al., 2017; Opoku-Baah and Wallace, 2020). Overall, results were consistent with a reduction of multisensory interaction for the deprived eye, in which the visual processing is strengthened following MD. Vice versa, an increased multisensory interaction for the non-deprived eye, in which visual processing is typically weakened, was found. Despite this behavioral evidence, whether a short period of deprivation alters neural correlates of multisensory interaction is still unknown. To fill this gap, we exploited the model of MD to induce short-term plasticity and investigated audio-visual processing. We combined psychophysical and electrophysiological approaches. To elicit a multisensory percept, we employed the *sound-induced flash illusion*, in which the number of perceived flashes can be biased by the number of co-occurring beeps (Shams et al., 2000; Hirst et al., 2020). We determined the impact of MD on neural correlates of audio-visual processing by measuring neural oscillations occurring in response to *fission* illusion trials. This illusion, in which a single flash coupled with two beeps leads to the perception of two flashes, reveals the impact of auditory input on visual temporal sensitivity in case of audio-visual conflicts. We also measured neural changes in visual processing to control that MD was successful (i.e., increasing excitability for the deprived eye) and to compare temporal and spectral profiles of visual and putative audio-visual effects elicited by MD.

* Corresponding author.
E-mail address: alessandra.federici@imtlucca.it (A. Federici).

https://doi.org/10.1016/j.neuroimage.2023.120141.
Received 21 December 2022; Received in revised form 21 April 2023; Accepted 27 April 2023
Available online 28 April 2023.

We investigated neural oscillations as they reflect high and low neuronal excitability cycles and reveal perceptual organization in both visual (Jensen et al., 2014; VanRullen, 2016) and multisensory processing (Cooke et al., 2019; Lennert et al., 2021). For the deprived eye, we expected MD to induce a reduction in alpha activity during visual processing, indexing the increased visual system excitability (Lunghi et al., 2015a). Moreover, we hypothesized MD to alter responses in the gamma range. Gamma activity has been associated with excitatory-inhibitory balance (Jensen et al., 2010; 2012), and its modulation was reliably linked with fission illusion perception (Bhattacharya et al., 2002; Mishra et al., 2007; Lange et al., 2011, 2013; Balz et al., 2016).

Neural oscillations can be distinct in evoked and induced components. Evoked oscillations are time and phase-locked to the onset of an external event, while induced oscillations are prompted by a stimulus but are not time- and phase-locked to its onset (Galambos, 1992, see also Keil et al., 2022). These distinct components of neural oscillations characterize different types of processing according to the direction of information flow: while the evoked activity has mainly been associated with feedforward processing (thalamo-cortical, Tallon-Baudry and Bertrand, 1999; Lakatos et al., 2009; Chen et al., 2012), the induced oscillatory activity has been linked to feedback processing (cortico-cortical connectivity, Pfurtscheller and Silva, 1999; Tallon-Baudry and Bertrand, 1999; Chen et al., 2012). Crucially, human and non-human animal model studies demonstrated that sensory deprivation primarily affects induced oscillatory activity (Bottari et al., 2016; Yusuf et al., 2017; Bednaya et al., 2021). Thus, the second goal of the paper was to assess which component of neural oscillations would be altered by short-term sensory deprivation. As homeostatic plasticity is an intrinsic feedback mechanism (Turrigiano and Nelson, 2004), we predicted to observe changes in induced oscillatory activity following temporary MD.

2. Materials and methods

2.1. Participants

Since the effect of MD on multisensory processing was unknown, we estimated the minimum sample size needed to reach the expected effect of MD on visual processing as previously reported in the literature. We expected the MD effect on visual processing to be at occipito-parietal electrodes, in the alpha range [8–14 Hz] (Lunghi et al., 2015a), and within the first stages of visual processing [0–120 ms] (comprising the earliest visual evoked potential, C1 wave, known to be modulated by MD; Lunghi et al., 2015a). The power analysis was performed by simulating our planned analysis (Post minus Pre Deprived eye vs. Post minus Pre Non-deprived eye) on the alpha frequency power using a cluster-based permutation test (Wang and Zhang, 2021). The analysis revealed an estimated minimum sample size of 17 participants (for further details on sample size estimation see Supplementary Materials and Fig. S1). Note that previous studies investigating the effect of MD using EEG analyzed up to 16 participants (Lunghi et al., 2015a; Zhou et al., 2015; Schwenk et al., 2020).

To determine individual suitability for the *main experiment* (EEG experiment), twenty-seven potential participants completed a *preliminary behavioral assessment* (see the Section 2.3.2. below) to ensure that participants enrolled in the EEG experiment perceived the fission illusion. Perceiving this multisensory illusion was the main prerequisite since we aimed to investigate MD impact during multisensory processing. Particularly, participants had to meet the following inclusion criteria: (i) to perceive the *fission illusion* with the dominant eye (i.e., >20% illusory rate), and (ii) not to be completely biased by the sound in the illusory conditions (i.e., <95% illusory rate) leaving room to modulations. Out of twenty-seven young adults tested (mean age 28.22 ± 2.41 SD, twelve males, and fifteen females), six participants were excluded as they did not meet these inclusion criteria or could not comply with the experimental instructions (see Supplementary Materials). Out of the 21 participants who performed the *main experiment*, one further participant was excluded due to his poor behavioral performance (the number of errors was 3 SD above the group mean in the conditions in which only auditory stimuli were presented, i.e., the control conditions). The final sample included 20 young-adult participants (mean age 28.45 ± 2.67 SD, eight males, and twelve females). They all had normal or corrected-to-normal vision (visual acuity ≥ 8/10, see below Section 2.3.2. *Preliminary behavioral assessment*) and did not report hearing deficits or a history of neurological conditions. Since one EEG and one behavioral dataset from different participants went lost due to technical issues during acquisitions, the analyzed data sample included 19 behavioral and 19 EEG datasets.

The study was approved by the local Ethical Committee (Comitato Etico di Area Vasta Nord Ovest Regione Toscana protocol n. 24579). Each participant signed a written informed consent before taking part in the experiment. The experimental protocol adhered to the principles of the Declaration of Helsinki (2013).

2.2. Stimuli and apparatus

The experiment was performed in a dimly lit and sound-attenuated chamber (BOXY, B-Beng s.r.l., Italy). Participants were comfortably sitting in front of the apparatus, with their eyes at a distance of 60 cm from the monitor. Visual stimuli were presented on an LCD monitor (60 Hz refresh rate; 24.5 inches; 1920 × 1080 screen resolution), and audio stimuli were delivered via a single speaker (Bose® Companion 2, series III multimedia) located below the screen and aligned with its center. Stimuli were flashes and beeps. Both visual and audio stimuli were created using Matlab (The Mathworks, Inc. - version 2017b). The audio stimulus was a 7 ms quadratic beep with a 3.5 kHz frequency and a sampling rate of 44.1 kHz, which was presented at about 75 dB. The visual stimulus was a 2° diameter grey dot displayed 5° below the center of the screen for 17 ms (corresponding to 1 frame) on a black background. The contrast level of the grey dot was selected individually via a staircase procedure to elicit the fission illusion in about 50% of trials (Pérez-Bellido et al., 2015, see below Section 2.3.2. *Preliminary behavioral assessment*). Stimuli were delivered using E-Prime® software (version 2, Psychology Software Tools, Inc. www.pstnet.com). The Audio/Visual (AV) Device (Electrical Geodesics, Inc.) was employed to ensure accurate optimal synchronization between the presented stimuli and the recorded EEG traces.

2.3. Experimental design

The whole procedure consisted of two main parts performed on two separate days: a *preliminary behavioral assessment* and the *main experiment*, in which the dominant eye was deprived of patterned visual input using a translucent eye patch (see Supplementary Materials for details). In both the *preliminary behavioral assessment* and the *main experiment,* participants performed a *monocular visual discrimination task*; while one eye was stimulated, the other eye was occluded with the translucent eye patch.

2.3.1. Monocular visual discrimination task

Participants were asked to report the number of perceived flashes (0, 1, or 2) while task-irrelevant beeps (0, 1, or 2) were presented. Responses were given by pressing one of three keypad buttons using the right-hand fingers. In each trial, audio (A) and visual (V) stimuli could be presented coupled or isolated, constituting eight conditions: half conditions were unisensory and comprised single, or couples of visual or auditory events (V and VV; A and AA) and the other half were multisensory (coherent audio-visual stimulation: AV and AVAV; illusory audio-visual stimulation: AVA and VAV, for a schematic summary of all conditions see Supplementary Materials Fig. S3 panel b). Unisensory auditory trials (i.e., A and AA) represented control conditions. They were employed to ensure that participants correctly performed the task. The presentation order of the conditions was randomized.

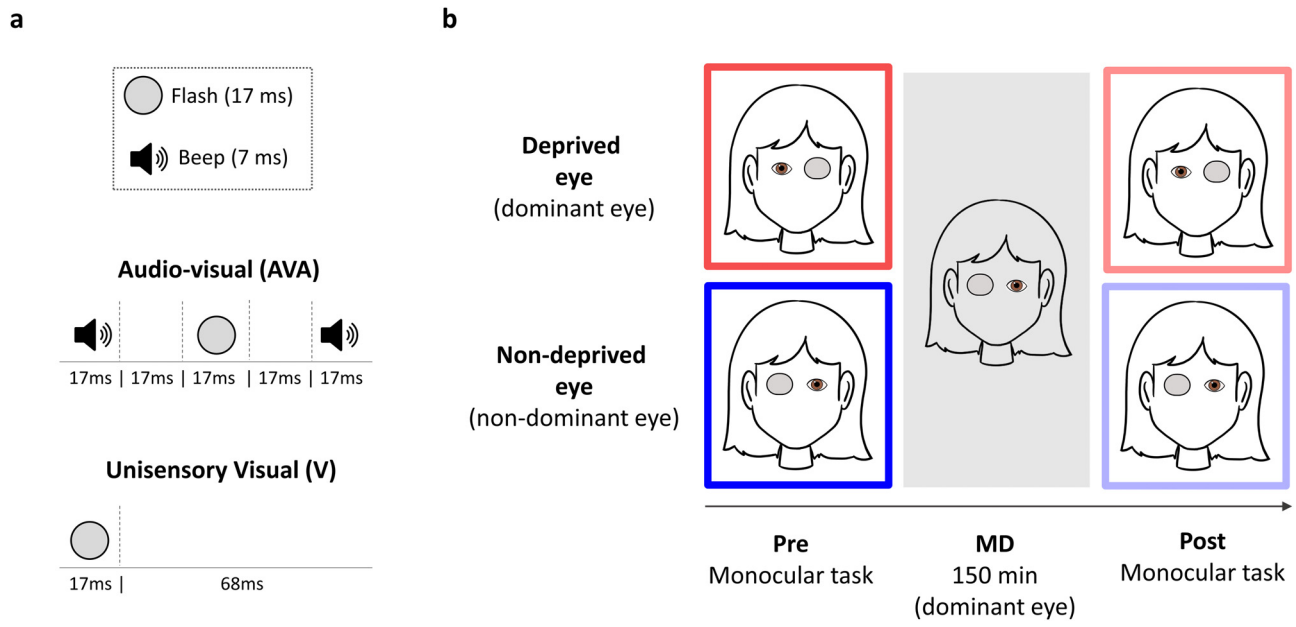

Fig. 1. Schematic illustration of the stimuli and the experimental design. (a) On the top, legend of the type of stimuli used. Below is the stimulation timeline for the multisensory AVA and unisensory V conditions (17 ms correspond to 1 frame). (b) Experimental design showing the four sessions performed with the Deprived eye (upper line, red contour) and the Non-deprived eye (bottom line, blue contour). In the Pre and Post deprivation phases, participants performed the visual monocular task with each eye (eye order was counterbalanced across participants). During the deprivation phase, participants wore translucent eye patch on the dominant eye (Deprived eye) for 150 min (MD phase). Monocular stimulation was achieved by patching the non-stimulated eye with the same translucent eye patch used for the deprivation.

Since our main aim was to explore changes in the neural response to audio-visual events caused by a short-term MD, the main analysis focused on the audio-visual condition inducing fission illusion (AVA). Generating an unstable percept, this illusion allows the investigation of subtle changes in audio-visual processing. Behavioral responses were fundamental to ensure the presence of the illusory percept. We investigated changes in the unisensory visual condition (V) as a control. Notably, the visual stimulus was the same single flash in AVA and V conditions.

All trials started with a grey fixation cross presented at the center of the screen on a black background. After 717 ms, the stimulation was delivered (see Fig. 1a for the stimulation timeline of V and AVA). Following the stimulation, a blank screen appeared for 500 ms (response-free time window). The fixation cross became white, and participants were asked to respond within 1 second (except for the staircase procedure, in which participants had infinite time to respond; see Section 2.3.2. *Preliminary behavioral assessment*). As soon as the response was given, a blank screen was presented for 300 ms before the beginning of the subsequent trial (see Fig. S3 panel a). Participants were asked to maintain their gaze at the fixation cross throughout the duration of the trial.

2.3.2. Preliminary behavioral assessment

To verify whether participant could take part in the *main experiment*, the ocular dominance via the Porta Test (see Supplementary Materials), the visual acuity via the eye chart, and the rate of the illusory percept during the *monocular visual discrimination task* were measured.

Once ocular dominance and visual acuity were tested, participants performed two short versions of the *monocular visual discrimination task*. The first short version comprised a staircase procedure (see Supplementary Materials for details) that was used to identify, at the individual level, the luminance contrast between the grey dot and the black background needed to elicit the fission illusion in about 50% of trials (Pérez-Bellido et al., 2015). Participants performed this test monocularly, with the dominant and non-dominant eye (the order was randomized). The contrast level for the dominant and non-dominant eye did not differ within-participant ($t(26)= -1.466$, $p = 0.155$). Then, the second short version of the *monocular visual discrimination task* (30 trials for each of the following conditions V, VV, AVA, VAV, A, and 6 for AA, AV, AVAV) was performed with the dominant eye (with the contrast identified by the staircase procedure) to evaluate whether the participant was fulfilling the inclusion criteria to take part in the *main experiment* (see Participants Section 2.1.).

Previous evidence revealed that individual sensory preference (*Audio* or *Visual*) impacts multisensory processing (Giard and Perronet, 1999). To assess whether individual sensory predisposition might affect multisensory short-term plasticity, participants monocularly performed a speeded object recognition task based on auditory, visual, and audio-visual information (see Supplementary Materials for details). Each participant's Sensory-Preference (*Audio* or *Visual*) was classified for each eye, and no significant difference was found between eyes (McNemar's test, $p>0.68$). Sensory-Preference was an additional measure that we considered: for this reason, the *Audio* and *Visual* groups' N was not balanced.

2.3.3. Main experiment

Participants recruited in the *main experiment* came to the laboratory a second time on a different day. Since the *main experiment* lasted about five hours, the data were always acquired in the morning (approximately between 9 am and 2 pm) to avoid possible confounds associated with the circadian cycle or related to (visual) activities performed before the experiment. Each participant repeated the short version of the *monocular visual discrimination task* with the dominant eye comprising the staircase procedure to ensure the test-retest reliability of the selected visual stimulus contrast (no significant difference was found between the contrast levels measured in the two assessments; $t(20)=0.637$, $p = 0.532$).

A brief practice of 16 trials was run before the *main experiment*. Participants performed the *monocular visual discrimination task*, with each eye, before (Pre) and after (Post) a period of monocular deprivation (MD) (see Fig. 1b) while their EEG signal was recorded. Thus, each participant performed a total of four sessions of the *monocular visual discrimination task* (i.e., at Pre and Post, both with the dominant and the non-dominant eye). Note that whether they started with the dominant

or the non-dominant eye was counterbalanced across participants. MD consisted of 150 min in which the dominant eye was occluded by the translucent eye patch, following a validated procedure (Lunghi et al., 2011). From now on, we will refer to the dominant eye as the 'Deprived eye' and the non-dominant eye as the 'Non-deprived eye'.

During the MD phase, participants were engaged in predefined activities to prompt, activate, and control multisensory interactions with the environment. Since the physical activity was demonstrated to boost short-term homeostatic plasticity in the adult visual cortex (Lunghi and Sale, 2015), all participants were engaged in the following activities: table football, table hockey, ping pong, and billiards, each of them lasting 15 min. Between each 15-minutes game about 3 min of rest were given to participants. Before and after the period comprising the games, participants had about 40 min of rest in which they were left free to engage in activities of their choice. Participants remained in the lab for the whole duration of the experiment, and the EEG cap was always kept on the scalp.

Each monocular session (i.e., Pre Deprived, Pre Non-deprived, Post Deprived, and Post Non-deprived) comprised 100 trials for the conditions V, VV, AVA, VAV, A, and 30 trials for the conditions AA, AV, AVAV, and was divided into five blocks (118 trials each) lasting about 5 min each. The number of trials was chosen to keep the duration of the monocular session within the estimated length of the MD effect (which has been demonstrated to be present for up to 90 min but substantially decreases after 15 min; see Lunghi et al., 2011).

2.4. EEG recording and preprocessing

EEG data were collected continuously during the four monocular task sessions (i.e., Pre Deprived, Pre Non-deprived, Post Deprived, and Post Non-deprived), using Electrical Geodesics EEG system with 64-channels (EGI; 500 Hz sampling rate). Offline, the data of the four sessions were concatenated at the individual level to detect common stereotypical artifacts. Data were preprocessed by implementing a validated approach (Stropahl et al., 2018; Bottari et al., 2020). The continuous recordings were filtered (low-pass cut-off at 40 Hz, Hanning filter, order 500; high-pass cut-off at 1 Hz, Hanning filter, order 100) and downsampled to 250 Hz to reduce the computational time. The filtered and downsampled data were segmented into consecutive 1-second epochs and cleaned using joint probability criterion: segments displaying an activity with a joint probability across all channels larger than 3 SD were removed (pop_jointprob function of EEGLAB; Delorme et al., 2007). Independent Component Analysis (ICA) based on the extended Infomax (Bell and Sejnowski, 1995; Jung et al., 2000a, 2000b) was then performed. The resulting ICA weights were saved and applied to the raw continuous unfiltered data (Stropahl et al., 2018; Bottari et al., 2020). Components associated with stereotypical artifacts, such as eye blinks and eye movements, were identified and removed using a semiautomatic procedure (CORRMAP, Viola et al., 2009). The data were then low-pass and high-pass filtered (100 Hz, filter order 100; 0.1 Hz, filter order 500) with a Hanning filter. Noisy channels were identified based on visual inspection and then interpolated using spherical spline interpolation (mean interpolated electrodes per subject 2.32 ± 2.26 SD) and re-referenced to the average. Finally, the residual power line fluctuations at 50 Hz were removed using the CleanLine EEGLAB plugin (https://github.com/sccn/cleanline). The single subject EEG data were then split again into the original four sessions. Each session was then segmented into epochs of 2.2 s, from −1 to 1.2 s with respect to the onset of the stimulation, and divided according to the condition (i.e., V and AVA). Note that the epoch length was the same for all conditions. Noisy epochs for each participant within each condition were then rejected based on the joint probability across channels (Delorme et al., 2007) with a threshold of 3 SD (mean number of trials retained for each subject in each session and used in the unisensory V condition: Pre Deprived 86.3 ± 4.6 SD, Pre Non-deprived 86.4 ± 6.3 SD, Post Deprived 85.0 ± 5.3 SD, and Post Non-deprived 86.7 ± 4.6 SD; in the multisensory AVA condition: Pre Deprived 86.6 ± 5.6 SD, Pre Non-deprived 85.7 ± 5.7 SD, Post Deprived 86.5 ± 5.0 SD, and Post Non-deprived 83.8 ± 6.4 SD). All these steps were performed with EEGLAB software (Delorme and Makeig, 2004). Data were then imported into Fieldtrip (Oostenveld et al., 2011) to perform time-frequency decomposition and statistical analyses.

2.5. Time-frequency decomposition

Time-frequency decomposition of the EEG data was performed within each session and separately for the visual and audio-visual conditions, following exactly the same approach for both conditions. Within each condition and session, we first extracted the induced power at a single trial level after subtracting the evoked activity (that is, subtracting from each trial the ERP computed averaging across trials without low-pass filtering). Time-frequency decomposition of single-trials was computed at each channel, separately for low (2–30 Hz) and high (30–80 Hz) frequency ranges (e.g., Lange et al., 2011). The oscillations in low frequencies were estimated using a Hanning taper with a frequency-dependent window length (4 cycles per time window) in steps of 2 Hz. Oscillations with higher frequencies were estimated using a Multitapers method with Slepian sequence as tapers, in steps of 5 Hz with a fixed-length time window of 0.2 s and fixed spectral smoothing of ± 10 Hz. For both frequency ranges, the power was extracted over the entire epoch (from −1 to 1.2 s) in steps of 0.02 s. Then, the average across trials was computed at the individual level within each session (Pre Deprived, Pre Non-deprived, Post Deprived, Post Non-deprived), conditions (V and AVA), and frequency range (low and high). The resulting oscillatory activity was baseline-corrected to obtain the relative signal change with respect to the baseline interval. The baseline was set between −0.7 and −0.3 s for the low-frequency range, and between −0.2 and −0.1 s for the high-frequency range. The low-frequency range, having longer cycles, required a wide baseline for the appropriate estimation of slow oscillations (Bottari et al., 2016, 2018). Moreover, the low-frequency baseline was kept temporally distant from the stimulus onset to avoid temporal leakage of post-stimulus activity into the baseline period (Cohen et al., 2014).

The same procedure, without ERP subtraction from single trials, was implemented to estimate the total power. The baseline-corrected evoked power was computed by subtracting the baseline-corrected induced power from the baseline-corrected total power.

2.6. Source reconstruction

To better characterize the neural alterations induced by MD, source estimation of the neural effects was performed using Brainstorm software (Tadel et al., 2011) on preprocessed EEG data. Sources were extracted by applying a dynamic statistical parametric mapping (dSPM; Dale et al., 2000), adopting minimum-norm inverse maps to estimate the locations of scalp electrical activities. For each dataset, we used single trials pre-stimulus baseline [− 0.1 to 0.002 s] to calculate single subject noise covariance matrices and to estimate individual noise standard deviations at each location (Hansen et al., 2010). The boundary element method (BEM) provided in OpenMEEG was adopted as a head model; the model was computed on the first dataset and then applied to all the others (default parameters in Brainstorm were selected). Source estimation was performed by selecting the option of constrained dipole orientations (Tadel et al., 2011). Time-frequency decomposition was computed for each participant on the estimated sources at the single-trial level using the same approach described for the time-frequency decomposition performed at the sensor level.

2.7. Statistical analysis

2.7.1. Behavioral data

Despite the focus of the study being to assess neural changes, we analysed behavioral measures to ensure that participants were actively

performing the task and they perceived the fission illusion, which was a study prerequisite.

For each participant, we computed the D-prime (d') as visual and audio-visual temporal sensitivity indices: d' = *z*(*p* hits) - *z*(*p* false alarms), where *z* is the inverse cumulative normal function, and *p* is the proportion of hits and false alarms out of signal and noise, respectively. Values equal to 0 or 1 were corrected as 1/n and (n-1)/n, respectively, with n being the number of signal or noise trials. To compute the visual d', we defined hits trials in which one flash is dispalyed (V condition) and participants correctly responded 'one'. Consequently, false alarms were trials in which two flashes were presented (VV), and participants responded to having seen one flash. To compute the audio-visual d', we defined, coherently with the fission illusion literature, false alarms AVA trials in which participants reported two flashes (Watkins et al., 2006; Whittingham et al., 2014; Pérez-Bellido et al., 2015; Vanes et al., 2016; Keil, 2020). Thus, AVAV trials in which participants correctly responded 'two flashes' were considered hits. Note that the audio-visual temporal sensitivity (d') is inversely related to the amount of fission illusion: smaller d' indicated a greater amount of illusory percepts and vice versa (note that Response means of each condition are reported in Supplementary Materials Fig. S4). To compute the d' we assessed that in visual and audio visual condition, as expected, the number of 'zero' responses was negligible (see Supplementary Materials).

Two mixed-design ANOVA, with Eye (Deprived and Non-deprived) and Time (Pre and Post) as within-subjects factors, and Sensory-Preference (*Audio* and *Visual*) in the Deprived eye and Sensory-Preference (*Audio* and *Visual*) in the Non-deprived eye as between-subjects factors, were performed separately on visual and audio-visual d' values. The Sensory-Preference between-subjects factors were inserted in order to control their impact on the visual and audio-visual perception.

2.7.2. C1 wave

First, we assessed whether we could replicate the modulatory effect of MD on the C1 wave, previously shown by Lunghi and colleagues (2015). We expected increased C1 amplitude in the Deprived eye and a decreased C1 in the Non-deprived eye after MD.

2.7.3. Neural oscillations

Oscillatory activity occurring after stimulus onset was analyzed separately for visual (V) and audio-visual (AVA) trials to assess MD impact on visual and audio-visual processing. Note that the same statistical approach was applied to visual and audio-visual conditions. Time-frequency analyses were separately performed for induced and evoked oscillatory activity for both low [4–30 Hz] and high [30–80 Hz] frequency ranges.

To assess the impact of MD, we subtracted the oscillatory activity recorded before MD from the oscillatory activity recorded after MD (i.e., Post minus Pre). This difference was computed separately for the Deprived and Non-deprived eyes. From now on, *PowChangeDeprived* represents relative changes in power due to MD for the Deprived eye, and *PowChangeNon-deprived* the relative changes in power due to MD for the Non-deprived eye.

To compare the impact of MD on the Deprived and Non-deprived eyes, a series of non-parametric cluster-based permutation tests (using paired t-statistics) were performed without a priori assumptions (i.e., across all electrodes, time-points, and frequencies) between *PowChangeDeprived* and *PowChangeNon-deprived*. This rather conservative statistical approach was chosen to highlight only signal changes that characterized visual and audio-visual MD effects. Cluster-based permutation tests were employed to control for multiple comparisons (Maris and Oostenveld, 2007). We used the Monte Carlo method with 1000 random permutations; cluster-level statistics were calculated taking the sum of the t-values within every cluster, with an alpha level of 0.05 (two-tailed) and a minimum neighbor channel = 1. Identified clusters were considered significant at $p<0.025$ (corresponding to a critical alpha level of 0.05 in a two-tailed test). We focused on the post-stimulus activity, and thus, statistical tests were performed for the entire response-free time window, that is, from 0 to 0.5 s. The time period after 0.5 s from the stimulation onset was discarded to prevent motor artifacts from being included. If a significant difference due to MD emerged in this test (*PowChangeDeprived* vs. *PowChangeNon-deprived*), we assessed whether differences between the two eyes emerged at Pre or Post. To this end, two planned comparisons (i.e., Pre Deprived vs. Pre Non-deprived and Post Deprived vs. Post Non-deprived) were performed using the same cluster-based permutation analysis approach and the same parameters reported above. In case a significant difference between Deprived and Non-deprived eye would emerge only at Post and not at Pre, it would be indicative of a specific effect of the MD manipulation and rule out possible differences between the two eyes at baseline.

2.7.4. Correlations between neural and behavioral changes

After assessing the normality of the data with Shapiro-Wilk tests ($p>0.05$), Pearson correlations were employed to assess whether the neural changes related to short-term MD were associated with behavioral changes. When compared, the correlations' results were contrasted using a bootstrap method adapted for independent samples (see https://github.com/GRousselet/blog/tree/master/comp2dcorr).

The datasets and code used in the present study are available from the corresponding author on reasonable request.

3. Results

3.1. Behavioral data

3.1.1. d prime (d')

3.1.1.1. Unisensory visual. The mixed-design ANOVA on visual d' with Eye (Deprived and Non-deprived) and Time (Pre and Post) as within-subjects factors and Sensory-Preference in the Deprived or in the Non-deprived eye as between-subjects factor revealed a significant main effect of Time ($F(1,15)=13.52$, $p = 0.002$). No main effects of Eye, Sensory-Preference in the Deprived or in the Non-deprived eye, nor other interaction effects were found (all $p>0.1$). These findings suggest a general decrease of temporal sensitivity at Post (mean d' ± SE for each session: Pre Deprived 1.44 ± 0.21; Post Deprived 1.13 ± 0.22; Pre Non-deprived 1.37 ± 0.26; Post Non-deprived 1.14 ± 0.23; see Fig. S5a).

3.1.1.2. Audio-visual. The mixed-design ANOVA performed on audio-visual d' revealed a significant main effect of Eye ($F(1,15)=7.53$, $p = 0.015$), showing that the Non-deprived eye was less susceptible to the fission illusion (mean d' ± SE for each session: Pre Deprived 0.58 ± 0.16; Post Deprived 0.53 ± 0.19; Pre Non-deprived 0.84 ± 0.23; Post Non-deprived 0.66 ± 0.17). A tendency towards significance emerged for the interaction between Eye, Sensory-Preference in the Deprived eye, and Sensory-Preference in the Non-deprived eye ($F(1,15)=4.01$; $p = 0.064$). This tendency might suggest that the participant's Sensory-Preference had an eye-specific impact; being an *Audio*-subject or a *Visual*-subject might affect the level of the fission illusion perceived with that eye (in the Deprived eye, mean d' ± SE A-group: 0.52 ± 0.19; V-group: 0.69 ± 0.20; in the Non-deprived eye A-group: 0.65 ± 0.20; V-group: 0.96 ± 0.36). No significant main effects of Time, Sensory-Preference in the Deprived or in the Non-deprived eye, nor other interactions emerged (all $p>0.08$). Notably, a strong fission illusion was elicited in both eyes, as highlighted by the small d' measured in each of the four sessions (see Supplementary Materials Fig. S5b). Since no main effect of the Sensory-Preference emerged neither in visual nor in audio-visual ANOVAs, the analyses of EEG activity were performed on the whole group.

3.1.2. Number of perceived flashes

We computed d' as it is an unbiased behavioral measure (Macmillan and Creelman, 2004). In the context of the employed task,

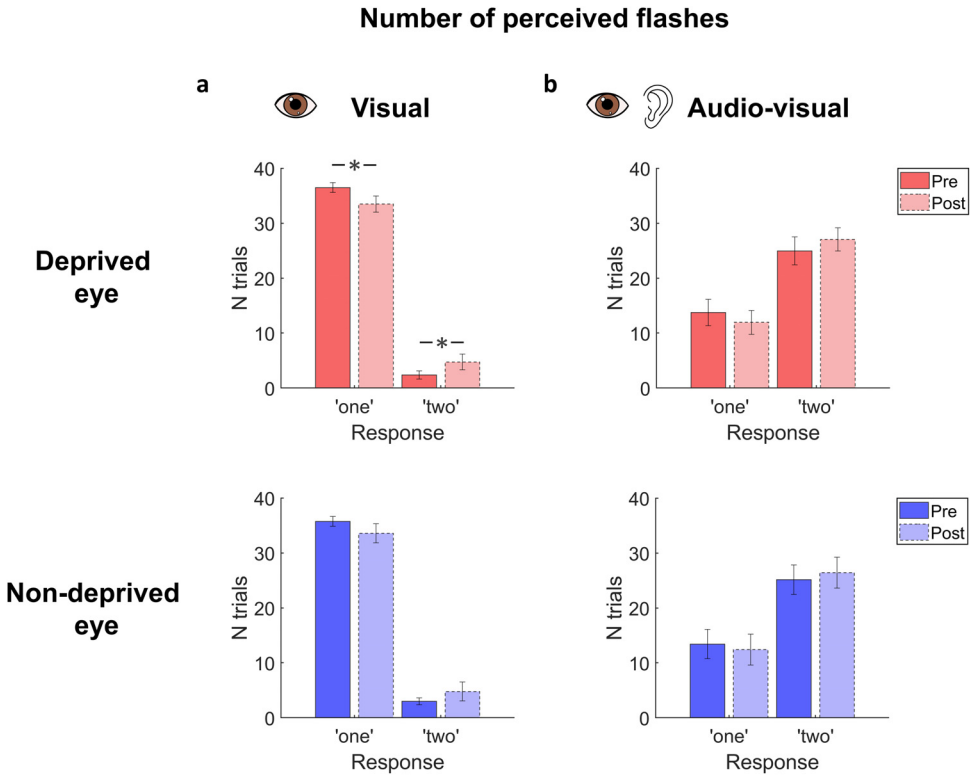

Fig. 2. Number of perceived flashes. The mean number of reported flashes, i.e., 'one' or 'two' responses, in the first two blocks are shown for the visual (V) and audio-visual (AVA) conditions (in a and b, respectively), for both the Deprived and Non-deprived eyes. In the visual condition, MD selectively affects the Deprived eye, inducing a decrease of 'one' responses (p = 0.011) and an increase of 'two' responses (p = 0.031). In the audio-visual condition, a higher number of 'two' responses indicates that the illusory percept dominates in both the Deprived and Non-deprived eyes before (Pre) and after (Post) the MD. Error bars represent the standard error of the mean.

the decrease in temporal sensitivity (d') means a reduction in the ability to report the number of presented flashes correctly. Thus, a reduction of temporal sensitivity could be due to an increased or decreased number of perceived flashes. For the visual condition (V), based on the expected enhanced excitability, we could predict a reduction of 'one' responses and an increase of 'two' responses in the Deprived eye after MD (see Lange et al., 2013 for an association between increased excitability and enhanced perception of two flashes).

3.1.2.1. Unisensory visual. To investigate whether the expected MD effect was elicited, we performed an additional analysis on correct responses in the unisensory V condition (when only one flash was presented) in the first two blocks. Only the first two blocks were considered as MD is known to be maximal within 10–15 min from deprivation (Lunghi et al., 2011). We calculated the number of 'one' responses and the number of 'two' responses for each eye (i.e., Deprived and Non-deprived) before and after MD (i.e., Pre and Post). Note that responses could also be 'zero', which would be the correct response for A and AA conditions. We then contrasted the number of 'one' responses in the Deprived eye between Pre and Post. The analysis revealed a significant decrease in 'one' responses after MD ($t(18)=2.854$; p = 0.011) and a significant increase in 'two' responses ($t(18)=-2.346$; p = 0.031; see Fig. 2a). No significant differences emerged for the Non-deprived eye (all $p>0.189$; when responses of all blocks were considered, results were substantially confirmed; see Supplementary Materials Fig. S6). These data revealed that MD increased the probability of perceiving two flashes when only one was presented to the Deprived eye.

3.1.2.2. Audio-visual. We performed the same analysis in the AVA condition (fission illusion). The analysis did not reveal any specific change in the type of response before vs. after MD, neither in the Deprived nor in the Non-deprived eye (all $p>0.182$; see Fig. 2b and Supplementary Materials Fig. S6). Overall, the data highlighted that a strong fission illusion was perceived with both eyes, as indicated by the fact that 'two' responses were more prominent than 'one' responses in all sessions.

3.2. C1 wave

Coherently with previous evidence (Lunghi et al., 2015a), the analysis revealed an increased C1 wave after MD for the Deprived eye, and the opposite for the Non-deprived eye (see Supplementary Materials for further details and Fig. S7)

3.3. Neural oscillations

To specifically investigate whether MD primarily affected feedback and/or feedforward connectivity, we assessed the impact of MD on induced and evoked neural oscillations associated with the processing of visual and audio-visual stimuli.

3.3.1. Unisensory visual

Induced power. The cluster-based permutation test performed on induced oscillatory activity within the low-frequency range [4–30 Hz] revealed a significant difference for *PowChangeDeprived* vs. *PowChangeNon-deprived* ($p<0.009$) spanning from occipital to frontal regions. MD elicited a marked decrease of induced activity in the alpha range [10–16 Hz] between 0 and 0.12 s (alpha synchronization period) selectively for the Deprived eye (see Fig. 3a, b). While no significant effects were found when comparing the oscillatory activity between the two eyes at Pre (all $p>0.51$), the comparison performed on induced oscillatory activity measured at Post revealed a significant difference ($p<0.002$) between the Deprived and Non-deprived eyes for the power in the alpha range [10–16 Hz]. These planned comparisons confirmed a direct effect of MD on alpha synchronization, and excluded possible confounds due to differences between the eyes at baseline. To further investigate the time-course of the MD effect in the alpha range, we assessed the difference between Post and Pre for each eye. For each session and participant, we extracted the mean induced alpha power [10–16 Hz] measured across three occipital electrodes (E36, E38, E40, which corresponded to the peak of the statistical effect in the *PowChangeDeprived* vs. *PowChangeNon-deprived* cluster-based permutation test). A series of paired t-tests were performed between Pre and Post for each eye, at each

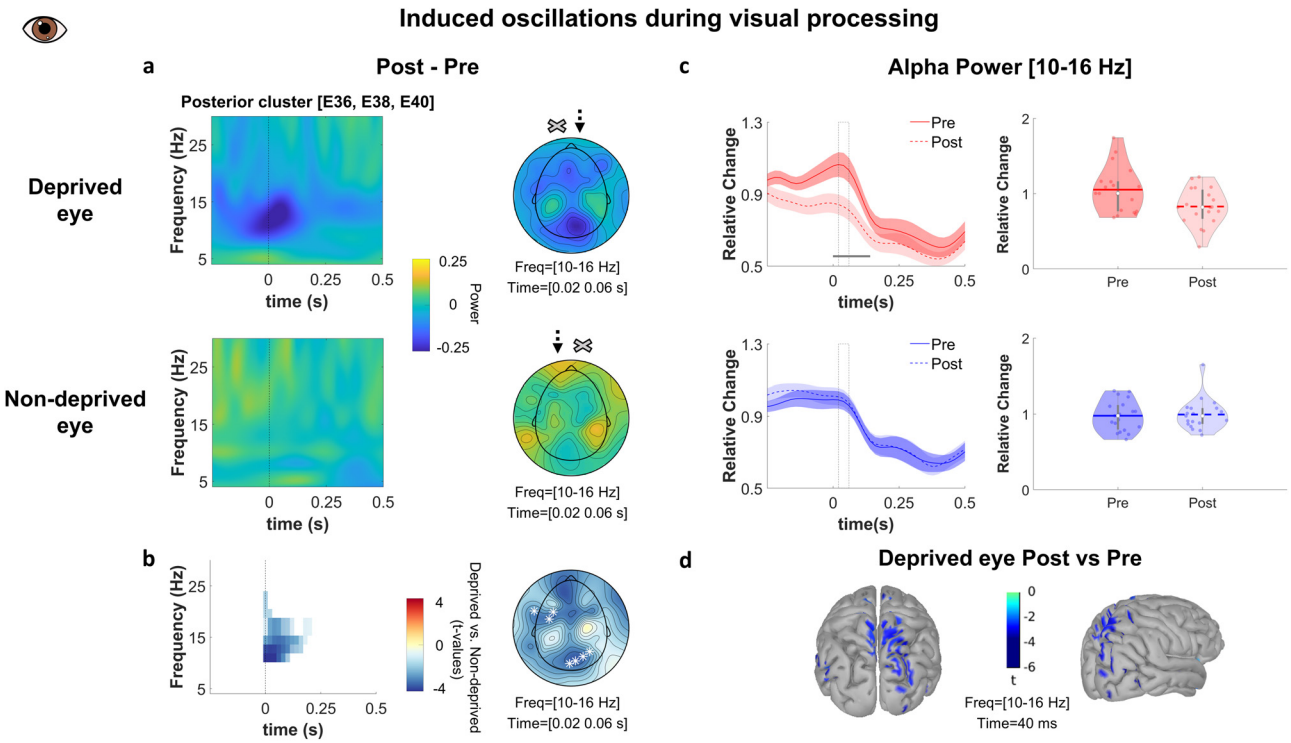

Fig. 3. The effect of Monocular Deprivation (MD) on visual processing, visual MD effect. (a) Induced oscillatory activity calculated as the difference between Post minus Pre at each eye: *PowChangeDeprived* (upper row) and *PowChangeNon-deprived* (bottom row) are plotted as a function of time [−0.25 - 0.5 s] and frequency [4–30 Hz]. The plots show the average across occipital electrodes (E36, E38, E40); 0 s indicates stimulus onset. Topographies in the alpha range [10–16 Hz] at a representative time window [0.02 - 0.06 s]; arrows indicate which eye was stimulated (here depicted a participant with right-eye dominance); crosses represent the eye covered by the translucent patch. (b) Statistical results. Time-frequency plot highlighting significant differences between *PowChangeDeprived* and *PowChangeNon-deprived* identified by the cluster-based permutation test (p<0.025, two-tailed) and the corresponding topography for the alpha range [10–16 Hz] at a representative time window [0.02 - 0.06 s]; electrodes belonging to the significant cluster are highlighted with white asterisks. (c) Time-course at the group level of the mean power in the alpha range [10–16 Hz] at Pre and Post (data are averaged across electrodes E36, E38, E40) separately displayed for the Deprived and the Non-deprived eye (upper and bottom rows); shaded areas represent the standard error of the mean; the continuous horizontal grey line indicates the significant difference between Pre and Post in the Deprived eye (from 0 to 0.14 s; p<0.05, FDR corrected). The dashed grey boxes represent the time window [0.02 - 0.06 s], comprising the alpha peak, in which the power in the alpha range [10–16 Hz] was extracted for each subject (across channels E36, E38, E40) and shown in the corresponding violin plots (right side; each dot represents individual data). (d) Source analysis performed to localize the visual MD effect; the image shows, at 40 ms after stimulus onset, the area in which the power in the alpha range [10 - 16 Hz] significantly decreased at Post with respect to Pre.

time-point within the whole-time window of interest [0–0.5 s] (FDR corrected, q = 0.05). A significant difference was found only for the Deprived eye, showing a clear decrease in the alpha synchronization after MD (from 0 to 0.14 s; for the Non-deprived eye all p>0.97; see Fig. 3c). Importantly, decreased alpha synchronization is coherent with previous findings showing the reversed pattern, i.e. increased alpha, during the desynchronization period (300–1000 ms; Lunghi et al., 2015a; see Supplementary Materials for a detailed explanation and Fig. S8).

No significant differences between *PowChangeDeprived* and *PowChangeNon-deprived* were found in the high-frequency range [30–80 Hz] (all p>0.67, see Fig. S9).

Evoked power. Cluster-based permutation analyses on evoked oscillatory activity were performed contrasting *PowChangeDeprived* vs. *PowChangeNon-deprived* to test whether MD alters feedforward visual processing. No significant differences emerged in either low or high frequencies (all p>0.13, see Fig. S10).

In sum, a visual MD effect emerged selectively for the Deprived eye and affected the induced oscillatory activity within the alpha range.

Source analysis. We investigated the electrical sources of the visual MD effect. To this end, a permutation paired t-test (1000 randomizations) was performed at the source level, on the power in the alpha range [10–16 Hz] between Pre and Post for the Deprived eye (time window [0–0.5 s]; FDR correction was applied on the time dimension). Results revealed that the visual MD effect was mainly located within the right hemisphere and comprised the superior parietal gyrus, the superior occipital gyrus, intraparietal and subparietal sulcus, and extended to calcarine sulcus (corrected p-threshold: 0.003; see Fig. 3d).

3.3.2. Audio-visual

After we assessed the impact of MD on unisensory visual processing (visual MD effect), we investigated whether MD can also affect audio-visual processing at the neural level. The induced and evoked oscillatory activities were tested separately within low and high-frequency ranges.

Induced power. The cluster-based permutation performed on induced oscillatory activity within the low-frequency range [4–30 Hz] between *PowChangeDeprived* and *PowChangeNon-deprived* showed no significant effects (all p>0.45, see Fig. S11). In contrast, the same analysis performed within the high-frequency range [30–80 Hz] revealed a significant effect in gamma activity (p<0.015). An increase in gamma activity [65–75 Hz] was found in the Non-deprived eye between 0.16 and 0.26 s, mainly in posterior electrodes (see Fig. 4a, b). The planned comparisons showed no significant effect at Pre (all p>0.07), while a significant difference between the two eyes emerged only at Post (p<0.022), confirming that MD specifically guided the effect. To further investigate the time-course of the induced gamma effect, we tested the difference between Pre and Post within each eye. For each session and participant, we extracted the mean induced gamma power [65–75 Hz] measured across two parieto-occipital electrodes (E40 and E42, which corresponded to the peak of the statistical effect in the *PowChangeDeprived* vs. *PowChangeNon-deprived* cluster-based permutation test). A series of

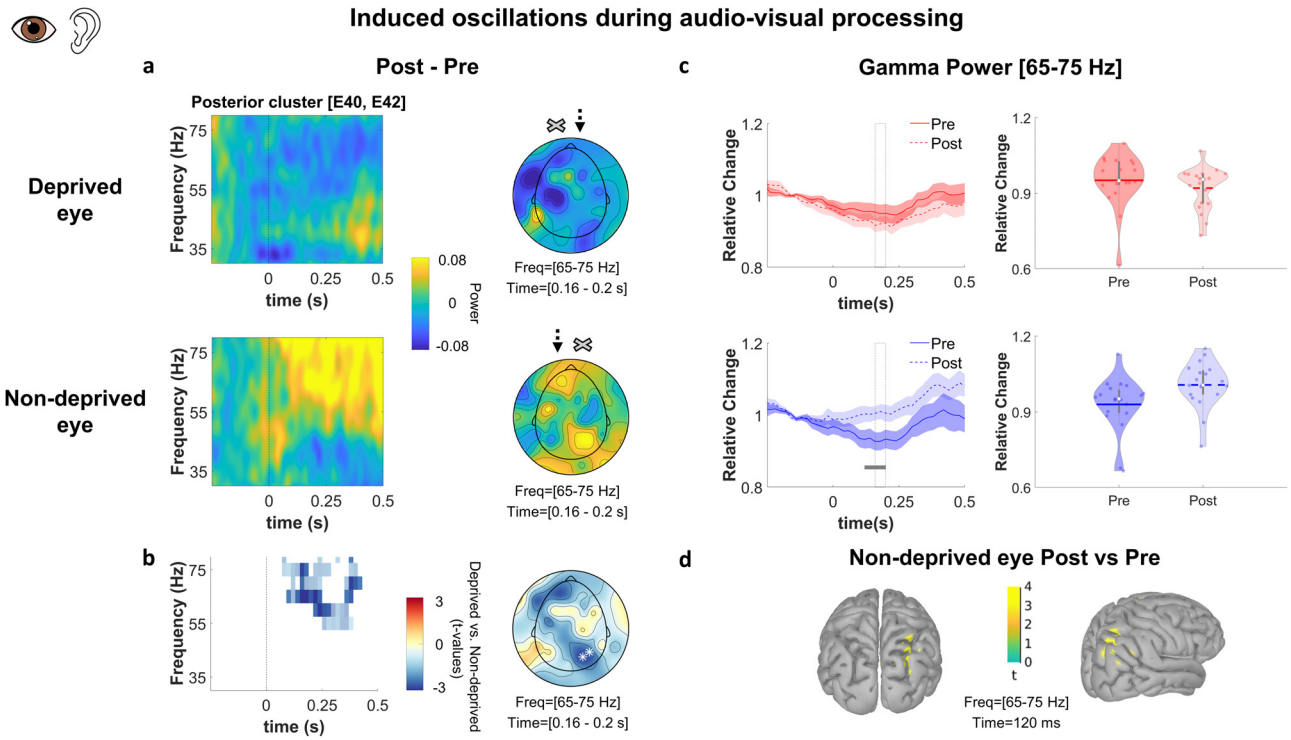

Fig. 4. The effect of Monocular Deprivation (MD) on audio-visual processing, audio-visual MD effect. (a) Induced oscillatory activity calculated as the difference between Post minus Pre at each eye: *PowChangeDeprived* (upper row) and *PowChangeNon-deprived* (middle row) are plotted as a function of time [−0.25 - 0.5 s] and frequency [30–80 Hz]. The plots show the average across posterior electrodes (E40, E42); 0 s indicates the stimulus onset. Topographies in the gamma range [65–75 Hz] at representative time window [0.16 - 0.2 s]; arrows indicate which eye was stimulated (represented in a participant with a right-eye dominance), and crosses represent the eye covered by the translucent patch. (b) Statistical results. Time-frequency plot highlighting significant differences between *PowChangeDeprived* and *PowChangeNon-deprived* identified by the cluster-based permutation test ($p<0.025$, two-tailed) and corresponding topography for the gamma range [65–75 Hz] at a representative time window [0.16 - 0.2 s]; electrodes belonging to the significant cluster are highlighted with white asterisks. (c) Time-course at the group level of the mean power in gamma range [65–75 Hz] at Pre and Post (data are averaged across electrodes E40, E42) separately displayed for the Deprived and the Non-deprived eye (upper and bottom rows); shaded areas represent the standard error of the mean; the continuous horizontal grey line indicates a significant difference between Pre and Post for the Non-deprived eye (from 0.12 to 0.2 s after stimulus onset; $p<0.05$, FDR corrected). The dashed grey boxes represent the time window [0.16 - 0.2 s] in which the power in the gamma range [65–75 Hz] was extracted for each subject (across channels E40 and E42) and shown in the corresponding violin plots (right side). (d) Source analysis performed to localize the audio-visual MD effect; the image shows at 120 ms after stimulus onset the area in which the power in the gamma range [65–75 Hz] significantly increases at Post with respect to Pre.

paired t-tests were performed between Pre and Post for each eye, at each time-point within the whole-time window of interest [0–0.5 s] (FDR corrected, $q = 0.05$). Only for the Non-deprived eye, a significant effect was found (from 0.12 to 0.2 s; for Deprived eye all $p>0.5$; see Fig. 4c).

Evoked power. When the difference between *PowChangeDeprived* and *PowChangeNon-deprived* was tested in the evoked power, no significant difference was found within the low-frequency range (all $p>0.09$) nor within the high-frequency range (all $p>0.05$, see Fig. S12).

To sum up, the audio-visual MD effect selectively emerged for the Non-deprived eye in the induced gamma power. Importantly, gamma activity was specific for audio-visual processing (i.e., it did not emerge for unimodal visual processing) and for the Non-deprived eye; therefore, we could exclude spurious ocular activity (e.g., microsaccades) as a primary driver of the effect. Muscular ocular activity should be non-specific, affect both eyes, and, most importantly, both visual and audio-visual processing. Instead, we hypothesized that this neurophysiological change could be driven by increased responsiveness to auditory inputs when the task is performed with the Non-deprived eye (see below Auditory upweighting Section 3.3.3.).

Source analysis. We investigated the sources of the audio-visual MD effect. To this end, a permutation paired *t*-test (1000 randomizations) was performed at the source level, on the power in the gamma range [65–75 Hz] between Pre and Post for the Non-deprived eye (time window [0–0.5 s]; FDR correction was applied on the time dimension). Results revealed that audio-visual MD effect was mainly located at the cortical level around the right intraparietal sulcus (corrected p-threshold: 0.002; see Fig. 4d).

3.3.3. *Auditory upweighting*

The gamma band increase during audio-visual processing in the Non-deprived eye following MD might suggest an upweighting of the auditory modality. If this would be the case, a greater neural response in the gamma range to unisensory acoustic stimulation (A and AA condition) should emerge selectively for the Non-deprived eye after MD. To this end, a hypothesis-driven ($p<0.05$, one tail) cluster-based permutation test was performed on the induced oscillatory activity in response to auditory stimuli (average across A and AA trials) in the high-frequency range [30–80 Hz] across all electrodes, frequencies, and time-points [0–0.5 s], between Pre and Post, separately in each eye (see Fig. 5a). The same preprocessing steps used for visual and audio-visual conditions were performed for auditory (A and AA) conditions. Mean trials number for each subject in each session used in the auditory analysis: Pre Deprived 111.4 ± 6.2 SD, Pre Non-deprived 113.1 ± 5.0 SD, Post Deprived 111.2 ± 5.4 SD, and Post Non-deprived 110.2 ± 6.1 SD. The analysis revealed a significant increase in gamma activity between 100 and 300 ms in response to auditory stimulation after MD ($p<0.04$), selectively for the Non-deprived eye (see Fig. 5b, c). Conversely, no significant difference emerged for the Deprived eye ($p>0.35$). This significant effect emerged in parietal electrodes as for the audio-visual MD effect (see Fig. 5b). These findings support our hypothesis that the increased

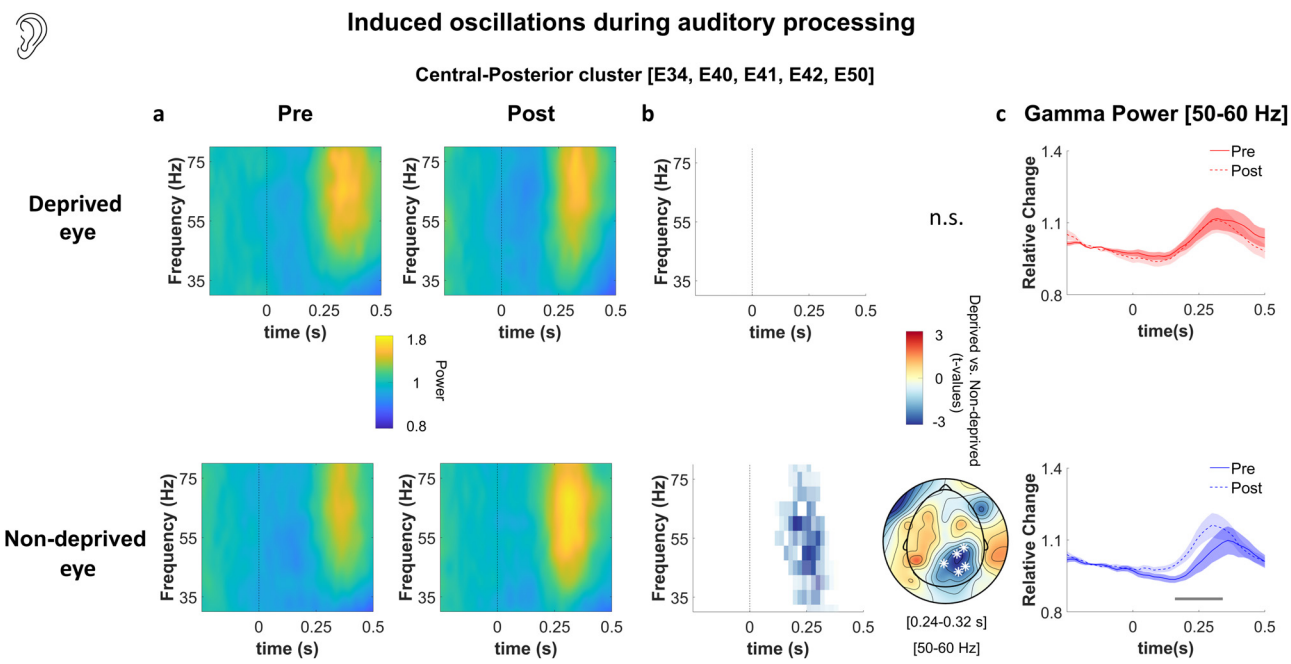

Fig. 5. Increased induced gamma activity for the Non-deprived eye after MD during auditory processing. (a) Induced oscillatory activity at Pre and Post are plotted as a function of time [−0.25 - 0.5 s] and frequency [30–80 Hz] for the Deprived (upper row) and Non-deprived eye (bottom row). The plots show the average across central-posterior electrodes (E34, E40, E41, E42, E50); 0 s indicates the stimulus onset. (b) Results of the cluster-based permutation test are shown in the time-frequency plots and highlight significant differences between Pre and Post, which emerged only for the Non-deprived eye. Topography shows the results of the cluster-based permutation test for the Non-deprived eye in the gamma range [50–60 Hz] over a representative time window [0.24 - 0.32 s]; white asterisks highlight significant electrodes (E34, E40, E41, E42, E50). (c) Time-course at the group level of the mean power in gamma range [50–60 Hz] at Pre and Post (data are averaged across electrodes E34, E40, E41, E42, E50), separately displayed for the Deprived and the Non-deprived eye (upper and bottom rows); shaded areas represent the standard error of the mean; the continuous horizontal grey line indicates a significant difference between Pre and Post for the Non-deprived eye (from 0.16 to 0.34 s after stimulus onset; $p<0.05$, FDR corrected).

induced gamma activity during audio-visual processing was due to an upweighting of auditory input.

Overall, the findings reveal a double dissociation concerning the neural effects of MD on visual and audio-visual processing. Decreased induced alpha synchronization in the Deprived eye during unisensory visual processing and increased induced gamma power for the Non-deprived eye during audio-visual processing (see Fig. 6a). Increased induced gamma activity was also found during unisensory auditory processing, supporting crossmodal upweighting selectively when the task is performed with the Non-deprived eye.

3.4. Association between neural and behavioral changes due to MD

Separately, for visual and audio-visual conditions, we investigated the degree of association between brain activity alterations and changes in behavioral performance. The average power at the frequencies of interest (alpha or gamma) was extracted within a time window and across channels that resulted significant in the cluster-based permutation tests (visual or audio-visual MD effects), and we computed the normalized difference between Post and Pre within each eye ([*PowChangeDeprived/Pre Deprived*] * *100;* [*PowChangeNon-deprived/Pre Non-deprived*] * *100*). Thus, within each condition (i.e., visual and audio-visual) and for each eye (i.e., Deprived and Non-deprived), we tested whether the power change (alpha or gamma) was correlated with the corresponding change in temporal sensitivity (difference in d' between Post and Pre sessions in the same condition and eye) using Pearson's correlation coefficient.

3.4.1. Unisensory visual

We tested whether the change of oscillatory activity in induced alpha power in the Deprived eye following MD (visual MD effect) was associated with a change in behavioral performance (i.e. change in visual temporal sensitivity). To this aim, we extracted the average power in the 10–16 Hz range between 0.02 and 0.06 s from the three significant electrodes (E36, E38, and E40) for each session. Then, the normalized Post-Pre difference of *PowChangeDeprived* and *PowChangeNon-deprived* was computed.

A significant positive correlation between normalized *PowChangeDeprived* (alpha power Post minus Pre) and visual temporal sensitivity change in the Deprived eye (visual d' Post minus Pre) was found ($r(16) = 0.492$, $p = 0.038$, see Fig. 6b). Following MD, the visual temporal sensitivity in the Deprived eye decreased in parallel with a reduction in induced alpha power in the same eye. We then assessed the same correlation between induced alpha change and visual temporal sensitivity change within the Non-deprived eye to control whether the correlation was selective to the Deprived eye; no significant effect was found for the Non-deprived eye ($p>0.99$).

3.4.2. Audio-visual

Next, we tested whether the increase in induced gamma after MD period (audio-visual MD effect) was associated with illusory fission percept (i.e., change in audio-visual temporal sensitivity). Thus, within each session, the induced power between 65 and 75 Hz was extracted within the 0.16–0.2 s time window and across the two significant posterior channels (E40 and E42). Then, the normalized Post-Pre difference of *PowChangeDeprived* and *PowChangeNon-deprived* was computed. No significant correlation was found neither for the Deprived eye nor for the Non-deprived eye (all $p>0.43$). However, at the behavioral level, a tendency for an interaction between illusion perception and sensory preferences was found ($F(1,15)=4.01$, $p = 0.06$), indicating that *Visual* subjects tended to experience less illusion than *Audio* subjects, especially in the Non-deprived eye (see Section 3.1.1.2. Audio-visual in the behavioral Results). Interestingly, the perception of the multisensory input partially depends on individual sensory predisposition (e.g., Giard

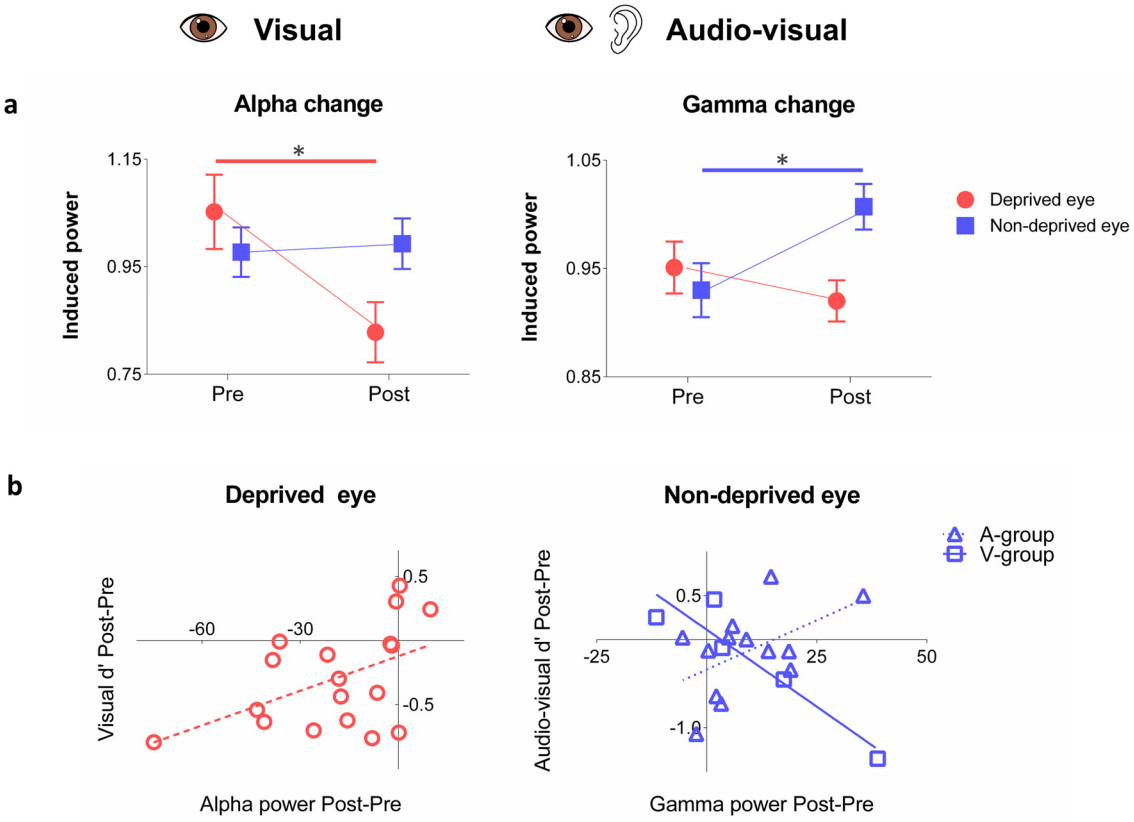

Fig. 6. Visual and audio-visual MD effects. a) The plots show the %normalized power change due to MD in unisensory visual and audio-visual processing. On the left, the visual MD effect: decreased induced alpha synchronization selectively for the Deprived eye (red) during unisensory visual processing. On the right, the audio-visual MD effect: enhanced induced gamma power selectively for the Non-deprived eye (blue) during audio-visual processing. Each dot represents the group mean and bars the standard error of the mean (cf. violin plots in Fig. 3c and 4c for individual data). Significant differences are highlighted with * (red indicates effect for the Deprived eye and blue for the Non-deprived eye). b) Correlations between neural change (Post minus Pre) and behavioral change in temporal sensitivity (d' Post minus Pre) for unisensory visual processing (left) and audio-visual processing (right).

and Perronet, 1999; Hong et al., 2021). Therefore, despite this not being the focus of this study, we additionally explored whether the association between neural and behavioral changes might be affected by individual sensory preference. Specifically, we calculated the correlation between *PowChangeNon-deprived* (gamma power Post minus Pre) and audio-visual d' change (Post minusPre) in the Non-deprived eye within *Audio* and *Visual* groups, classified according to participants' Sensory-Preference (estimated for the same eye). Pearson correlation revealed a significant negative correlation in the V-group ($r(3) = -0.937$; $p = 0.019$), while a tendency toward a significant positive correlation was found in the A-group ($r(11) = 0.513$; $p = 0.073$, see Fig. 6b). The two correlations significantly differed (difference=1.45 CI [0.17 1.80]. Since Pearson correlations were performed, the confidence interval was adjusted as described in Wilcox (2009); see Supplementary Materials Fig. S14). While these results are based on an explorative analysis and small sub-samples, they seem to suggest that the audio-visual MD effect might have a different impact on the illusory percept according to the participants' sensorypreference: in V-group, the increase of induced gamma activity in the Non-deprived eye was positively associated with a fission illusion increase (smaller d' after MD), while in A-group the increase of induced gamma activity seemed to be associated with a fission illusion decrease (larger d' after MD).

3.5. Relationship between the audio-visual and visual MD effects

To investigate the relationship between neural changes associated with audio-visual and visual processing we first performed a Pearson correlation between decreased induced alpha synchronization in the Deprived eye during unisensory visual processing and increased gamma power for the Non-deprived eye during audio-visual processing, which did not show any significant result ($r(17)=0.11$, $p = 0.65$).

We then explored whether behavioral temporal sensitivity and neural activity at baseline could help explain part of the variance. A more complex linear regression model was run. In the model we predicted for the Non-deprived eye the audio-visual gamma power after MD with the following factors: (i) the alpha power change (Post minus Pre) for the visual condition in the Deprived eye, (ii) the baseline (Pre) audio-visual gamma activity in each eye and (iii) the baseline (Pre) visual and audio-visual behavioral temporal sensitivity for the Deprived eye. The model was significant ($F(12)=3.41$, $p = 0.038$, Adjusted R-Squared: 0.415) and, results revealed that the larger the visual MD effect (alpha synchronization decreased Post-Pre) in the Deprived eye, the higher the gamma power during audio-visual processing for the Non-deprived eye after MD ($\beta=-2.481$, $p = 0.029$), linking the two neural changes. Moreover, higher visual temporal sensitivity (d') at baseline was associated with smaller gamma changes, i.e., less auditory upweighting ($\beta=-2.28$, $p = 0.042$). Finally, we observed a change of balance between audio-visual gamma at baseline (Pre) in the Deprived eye and audio-visual gamma response after MD (Post) in the Non-deprived eye ($\beta=2.990$, $p = 0.011$), possibly indicating a shift of audio-visual responsiveness across the two eyes.

4. Discussion

In this study, adult neural plasticity of both unisensory visual and multisensory audio-visual processes was investigated to assess whether

the impact of MD extends beyond visual processing. Induced and evoked oscillatory activity changes both in visual and audio-visual processing were measured after 150 min of altered visual experience (brief MD). Induced alpha synchronization associated with the early phase of visual processing (<150 ms) decreased after MD selectively for the Deprived eye. Conversely, induced gamma associated with audio-visual processing increased after MD only in the Non-deprived eye, within a later temporal window (~100–300 ms). Notably, main visual and audio-visual processing alterations were found for the induced component of neural oscillations. Source modeling linked both visual and audio-visual MD effects to the right parieto-occipital cortex. Our data reveal the specific neural signatures of temporary MD effects on visual and audio-visual processes and shed light on their shared feedback nature. We demonstrated that a brief period of monocular visual experience in adulthood specifically changes the neural response to multisensory audio-visual events because of plasticity in feedback connectivity.

4.1. Spectro-temporal properties of the visual MD effect

The observed visual MD effect is in line with previous studies (Lunghi et al., 2015a, 2015b; Zhou et al., 2015; Binda et al., 2018; Schwenk et al., 2020). The reduced alpha synchronization observed when the task was performed with the Deprived eye after MD is consistent with increased excitability to compensate for the absence of stimulation during the deprivation phase. This effect complements the alpha enhancement during desynchronization (Lunghi et al., 2015a, see Supplementary Materials for further details, Fig. S8). Source modeling suggested that the alpha reduction was mainly localized in the right hemisphere in superior parieto-occipital areas, with some activities extending to primary visual areas (calcarine sulcus). These results confirm the modulation of alpha rhythm induced by short-term plasticity, previously shown in the frequency domain as a change in alpha peak amplitude (Lunghi et al., 2015a), and characterize the spectro-temporal properties of this neural effect. Namely, a selective decrease of alpha synchronization [10–16 Hz] occurs in the early stages of visual processing (<150 ms). Notably, major changes elicited by MD emerged for the induced oscillatory activity (i.e., not phase-locked to stimulus onset), suggesting an important role of feedback connectivity on short-term visual plasticity. However, changes were also measured in early components (C1 wave) of the visual evoked potentials (VEPs; see Fig. S7 in Supplementary Materials), indicating a role of phase-locked neural processing as well. Overall, these results are coherent with spectroscopy data showing an increase of excitability in the early visual cortex as indicated by reductions of inhibitory gamma-aminobutyric acid (GABA) concentration after short-term MD (Lunghi et al., 2015b). Moreover, selectively for the Deprived eye, a significant correlation was found between decreased induced alpha synchronization and changes in behavioral performance after MD, suggesting a potential link between this neural change and the ability to discriminate temporal aspects of visual processing.

4.2. The impact of MD on audio-visual processing

Previous behavioral studies have shown that multisensory perception can be altered by MD (Lo Verde et al., 2017; Opoku-Baah and Wallace, 2020). By measuring changes in neural oscillations, we assessed neural mechanisms underpinning multisensory short-term plasticity and revealed the specific enhancement of induced gamma activity [65–75 Hz] selectively for the Non-deprived eye when processing audio-visual input. The audio-visual MD effect involved the right intraparietal sulcus, suggesting its central role in short-term plasticity induced by MD.

We hypothesized that the audio-visual MD effect could be due to a crossmodal upweighting of the other modality (i.e., audition). To this end, we tested whether the neural response to unisensory auditory stimuli was increased following MD in each eye. The observation that gamma response to auditory input increased following MD selectively for the Non-deprived eye confirmed our hypothesis. This result revealed that short-term plasticity following MD alters both visual and auditory neural representations. Interestingly, alterations of neural excitability due to temporary binocular deprivation were previously shown to increase heteromodal responses in the visual cortex (Merabet et al., 2008).

From a neurophysiological perspective, it is important to remark that neural profiles of short-term plasticity following MD seem to depend on the type of input at hand. While the visual stimulus was the same in visual and audio-visual conditions, short-term plasticity was characterized by specific oscillatory fingerprints (Siegel et al., 2012): alpha decreased during visual processing while gamma increased during audio-visual, as well as during auditory processing.

To what extent does this neural alteration interact with individuals' sensory predisposition? In the Non-deprived eye, the correlation between enhanced gamma activity in audio-visual processing and behavioral performance seems to indicate opposite MD impacts on illusory perception with respect to participants' Sensory-Preference. Although preliminary, this result opens the possibility that the upweighting of auditory information during audio-visual processing after MD affects visual perception according to individual sensory preference. Coherently with the extreme flexibility and adaptability of multisensory functions (Giard and Perronet, 1999; Fujisaki et al., 2004; Van Atteveldt et al., 2014), the perception of the multisensory input after MD might change as a function of individual sensory predisposition. This inference should be further verified with psychophysics experiments (see Rohe et al., 2019), designed to directly estimate auditory modality's weight changes during audio-visual processing after MD. Interestingly, a recent study investigating cross-modal recalibration highlighted how individual variability in one sensory modality (visual reliability) differently affects recalibration of the other modality (audition, Hong et al., 2021).

Binocular input was shown to be critical for developing audio-visual perception: anomalies in different audio-visual perceptual tasks were reported in cases of monocular enucleation (Moro and Steeves, 2018a, 2018b), individuals affected by early monocular cataracts (Chen et al., 2017), and people suffering from amblyopia (Narinesingh et al., 2015, 2017; Richards et al., 2017). The present results, revealing that MD induces short-term plasticity of audio-visual processing, encourage possible treatments of audio-visual anomalies associated with MD. Increasing evidence in animal studies supports clinical treatment of adult amblyopia (Hensch and Quinlan, 2018), and crucially a recent study conducted with adult people affected by amblyopia has shown that MD combined with physical exercise could be a promising intervention to promote visual recovery (Lunghi et al., 2019). Future studies might help understand whether multisensory audio-visual processing could also benefit from this novel clinical treatment.

4.3. The pivotal role of induced cortical response in experience-dependent plasticity

Both visual and audio-visual MD effects were found in induced neural oscillations, likely reflecting main alterations in feedback processing integrating sensory input and ongoing cortical activity (Galambos 1992; Klimesch et al., 1998; Tallon-Baudry and Bertrand, 1999; Chen et al., 2012; Keil et al., 2022).

Visual MD effect was found in the induced alpha band, which was previously demonstrated to be drastically impaired by the transient absence of visual experience during development (Bottari et al., 2016). Animal studies involving congenital deaf cats demonstrated that mainly induced, and not evoked, oscillatory activity in the primary auditory cortex is extremely reduced across a wide range of frequency bands (e.g., Yusuf et al., 2017). The authors hypothesized that the absence of sensory stimulation prevents the development of neural mechanisms allowing the integration of sensory signals and internal representations. Evidence

of alterations of induced oscillatory activity following sensory deprivation was reported not only within modality, for visual (Bottari et al., 2016) and auditory systems (Yusuf et al., 2017), but also cross-modally. In humans, early-onset deafness selectively affects induced oscillatory activity associated with visual processing (Bednaya et al., 2021). The present audio-visual MD effect (increased induced gamma activity) provides evidence in the same direction also for multisensory processing. Taken together, this evidence suggests a substantial alteration of cortico-cortical feedback activities, in case of sensory input absence in both developmental and adult brain, for unisensory and multisensory functions. This is in line with previous evidence suggesting that the plasticity of feedback connectivity represents an extremely flexible mechanism to process sensory information according to changing demands (Polley et al., 2006).

4.4. Limitations of the study

The visual MD effect is usually assessed with binocular rivalry in which the two eyes are tested in competition (e.g., Lunghi et al., 2011). By employing a task to measure audio-visual processing monocularly we were not in the position to assess ocular dominance and thus fully replicate previous findings. Direct behavioral impact of MD on monocular visual processing is still poorly understood: while some results have highlighted significant changes (e.g., contrast threshold: Zhou et al., 2013), others have reported no change (temporal synchrony: Chen et al., 2020; and contrast increment threshold: Wang et al., 2020). While in the present study, some evidence emerged that MD altered the ability to discriminate temporal characteristics of visual inputs, further psychophysical studies are required to confirm results.

Conversely, while convincing evidence emerged at the neural level, no behavioral effects on audio-visual processing occurred. One possible explanation comes from the small disparity between audio and visual stimuli (only one or two events each; see Rohe et al., 2019). Given the time constraints intrinsic to the MD effect (Lunghi et al., 2011), it was impossible to test conditions with larger audio-visual disparity (that is, all combinations across one to four flashes and beeps, as in Rohe et al., 2019). Moreover, it is also possible that the inter-subject variability driven by opposite sensory preferences might have hindered the effect. While this interaction seems of interest in explaining interindividual variability, a larger sample with a balanced number of subjects with visual and auditory sensory preferences is needed to confirm these intriguing preliminary results on how multisensory plasticity could be affected by individual sensory predisposition.

While a clear strength reduction of the Non-deprived eye (i.e., increased alpha synchronization) did not emerge, this is in line with the literature. The strongest impact of MD is known to be on the Deprived eye, while the opposite effect on the Non-deprived eye was found to be much smaller (Lunghi et al., 2015a; Binda et al., 2018) or even absent (Zhou et al., 2015). Thus, larger sample sizes may be required to measure neural effects on the Non-deprived eye during visual processing. Further studies might help to assess whether depriving the non-dominant eye will lead to the same MD effects. However, given the absence of difference at Pre, we can rule out the possibility that our effects are due to baseline differences between the dominant and the non-dominant eye. Noticeably, the visual MD effect emerged here for the Deprived eye, while the audio-visual MD effect emerged only for the Non-deprived eye. While these effects are in line with previous behavioral studies (Lo Verde et al., 2017; Opoku-Baah and Wallace, 2020), they also support the crucial role of MD in inducing flexible alterations of interocular excitability balance and, in turn, in audio-visual processes. Moreover, although an interaction between MD and eye dominance cannot be excluded, a recent study reported that the MD effect was the same regardless of whether the dominant or the non-dominant eye was deprived (Schwenk et al., 2020).

5. Conclusions

These results demonstrated that a brief period of monocular visual experience in adulthood is able to change the neural response not only to visual stimuli but also to multisensory events. The data unveiled the spectral fingerprints of adult short-term plasticity induced by a brief period of MD for visual and audio-visual processing. We found enhanced excitability (i.e., decreased induced alpha synchronization) for the Deprived eye during an early phase of visual processing, and we demonstrated the presence of neural alterations beyond the visual processing. Induced gamma activity associated with audio-visual processing was increased by MD at a later latency and only when the task was performed with the Non-deprived eye. The analyses of responses to unisensory auditory input indicate an upweighting of sound input following MD, selectively for the Non-deprived eye. Importantly, these distinct neural effects were found in the induced neural oscillations, revealing that experience-dependent plasticity involves alterations in feedback processing not only during development but also in adulthood. This observation is consistent with the existence of a general mechanism shared across sensory modalities and life cycle.

Funding

This work was supported by PRIN 2017 research grant (Prot. 20177894ZH) to Davide Bottari.

Declaration of Competing Interest

The authors declare no competing financial interests.

Credit authorship contribution statement

Alessandra Federici: Conceptualization, Investigation, Data curation, Formal analysis, Writing – original draft, Writing – review & editing. **Giulio Bernardi:** Conceptualization, Writing – review & editing. **Irene Senna:** Formal analysis, Writing – review & editing. **Marta Fantoni:** Investigation. **Marc O. Ernst:** Formal analysis, Writing – review & editing. **Emiliano Ricciardi:** Resources, Writing – review & editing. **Davide Bottari:** Conceptualization, Investigation, Data curation, Formal analysis, Writing – original draft, Writing – review & editing, Supervision, Project administration, Funding acquisition.

Data availability

The datasets and code used in the present study are available from the corresponding author on reasonable request.

Acknowledgments

We would like to thank Cesare V. Parise for the helpful discussion and feedback regarding data analysis.

Supplementary Materials

Supplementary material associated with this article can be found, in the online version, at doi:10.1016/j.neuroimage.2023.120141.

References

Balz, J., Keil, J., Roa Romero, Y., Mekle, R., Schubert, F., Aydin, S., Ittermann, B., Gallinat, J., Senkowski, D., 2016. GABA concentration in superior temporal sulcus predicts gamma power and perception in the sound-induced flash illusion. Neuroimage 125, 724–730.

Bednaya, E., Pavani, F., Ricciardi, E., Pietrini, P., Bottari, D., 2021. Oscillatory signatures of Repetition Suppression and Novelty Detection reveal altered induced visual responses in early deafness. Cortex.

Bell, A.J., Sejnowski, T.J., 1995. An information-maximization approach to blind separation and blind deconvolution. Neural Comput. 7, 1129–1159.

Bhattacharya, J., Shams, L., Shimojo, S., 2002. Sound-induced illusory flash perception: role of gamma band responses. Neuroreport 13, 1727–1730.
Binda, P., Kurzawski, J.W., Lunghi, C., Biagi, L., Tosetti, M., Morrone, M.C., 2018. Response to short-term deprivation of the human adult visual cortex measured with 7T bold. Elife 7, 1–25.
Bottari, D., Bednaya, E., Dormal, G., Villwock, A., Dzhelyova, M., Grin, K., Pietrini, P., Ricciardi, E., Rossion, B., Röder, B., 2020. EEG frequency-tagging demonstrates increased left hemispheric involvement and crossmodal plasticity for face processing in congenitally deaf signers. Neuroimage 223, 117315.
Bottari, D., Kekunnaya, R., Hense, M., Troje, N.F., Sourav, S., Röder, B., 2018. Motion processing after sight restoration: no competition between visual recovery and auditory compensation. Neuroimage 167, 284–296.
Bottari, D., Troje, N.F., Ley, P., Hense, M., Kekunnaya, R., Röder, B., 2016. Sight restoration after congenital blindness does not reinstate alpha oscillatory activity in humans. Sci. Rep. 6.
Castaldi, E., Lunghi, C., Morrone, M.C., 2020. Neuroplasticity in adult human visual cortex. Neurosci. Biobehav. Rev. 112, 542–552.
Chen, C.C., Kiebel, S.J., Kilner, J.M., Ward, N.S., Stephan, K.E., Wang, W.J., Friston, K.J., 2012. A dynamic causal model for evoked and induced responses. Neuroimage 59, 340–348.
Chen, Y.C., Lewis, T.L., Shore, D.I., Maurer, D., 2017. Early Binocular Input Is Critical for Development of Audiovisual but Not Visuotactile Simultaneity Perception. Curr. Biol. 27, 583–589.
Chen, Y., Min, S.H., Cheng, Z., Chen, S., Wang, Z., Tao, C., … Zhou, J., 2020. Short-term deprivation does not influence monocular or dichoptic temporal synchrony at low temporal frequency. Front. Neurosci. 14, 402.
Cohen, M.X., 2014. Analyzing Neural Time Series data: Theory and Practice. MIT press.
Cooke, J., Poch, C., Gillmeister, H., Costantini, M., Romei, V., 2019. Oscillatory properties of functional connections between sensory areas mediate cross-modal illusory perception. J. Neurosci. 39, 5711–5718.
Dale, A.M., Liu, A.K., Fischl, B.R., Buckner, R.L., Belliveau, J.W., Lewine, J.D., Halgren, E., 2000. Dynamic statistical parametric mapping: combining fMRI and MEG for high-resolution imaging of cortical activity. Neuron 26, 55–67.
Delorme, A., Makeig, S., 2004. EEGLAB: an open source toolbox for analysis of single-trial EEG dynamics including independent component analysis. J. Neurosci. Method. 134, 9–21.
Delorme, A., Sejnowski, T., Makeig, S., 2007. Enhanced detection of artifacts in EEG data using higher-order statistics and independent component analysis. Neuroimage 34, 1443–1449.
Espinosa, J.S., Stryker, M.P., 2012. Development and plasticity of the primary visual cortex. Neuron 75, 230–249.
Fujisaki, W., Shimojo, S., Kashino, M., Nishida, S., 2004. Recalibration of audiovisual simultaneity. Nat. Neurosci. 77 (7), 773–778.
Galambos, R., 1992. A comparison of certain gamma band (40-Hz) brain rhythms in cat and man. In: Induced Rhythms in the Brain. Birkhäuser, Boston, MA, pp. 201–216.
Giard, M.H., Peronnet, F., 1999. Auditory-visual integration during multimodal object recognition in humans: a behavioral and electrophysiological study. J. Cogn. Neurosci. 11, 473–490.
Hansen, P., Kringelbach, M., Salmelin, R., 2010. MEG: An Introduction to Methods. Oxford University Press (OUP).
Hensch, T.K., Quinlan, E.M., 2018. Critical periods in amblyopia. Vis. Neurosci. 35, E014.
Hirst, R.J., McGovern, D.P., Setti, A., Shams, L., Newell, F.N., 2020. What you see is what you hear: twenty years of research using the Sound-Induced Flash Illusion. Neurosci. Biobehav. Rev. 118, 759–774.
Hong, F., Badde, S., Landy, M.S., 2021. Causal inference regulates audiovisual spatial recalibration via its influence on audiovisual perception. PLoS Comput. Biol. 17 (11), e1008877.
Jensen, O., Bonnefond, M., VanRullen, R., 2012. An oscillatory mechanism for prioritizing salient unattended stimuli. Trend. Cogn. Sci. 16, 200–206.
Jensen, O., Gips, B., Bergmann, T.O., Bonnefond, M., 2014. Temporal coding organized by coupled alpha and gamma oscillations prioritize visual processing. Trend. Neurosci. 37, 357–369.
Jensen, O., Mazaheri, A., 2010. Shaping functional architecture by oscillatory alpha activity: gating by inhibition. Front. Hum. Neurosci. 186.
Jung, T.P., Makeig, S., Humphries, C., Lee, T.W., McKeown, M.J., Iragui, V., Sejnowski, T.J., 2000a. Removing electroencephalographic artifacts by blind source separation. Psychophysiology 37, 163–178.
Jung, T.P., Makeig, S., Westerfield, M., Townsend, J., Courchesne, E., Sejnowski, T.J., 2000b. Removal of eye activity artifacts from visual event-related potentials in normal and clinical subjects. Clin. Neurophysiol. 111, 1745–1758.
Karmarkar, U.R., Dan, Y., 2006. Experience-dependent plasticity in adult visual cortex. Neuron 52, 577–585.
Keil, J., 2020. Double flash illusions: current findings and future directions. Front. Neurosci. 14, 1–8.
Keil, A., Bernat, E.M., Cohen, M.X., Ding, M., Fabiani, M., Gratton, G., … Weisz, N., 2022. Recommendations and publication guidelines for studies using frequency domain and time-frequency domain analyses of neural time series. Psychophysiology 59 (5), e14052.
Klimesch, W., Russegger, H., Doppelmayr, M., Pachinger, T., 1998. A method for the calculation of induced band power: implications for the significance of brain oscillations. Electroencephalogr. Clin. Neurophysiol. 108, 123–130.
Lakatos, P., O'Connell, M.N., Barczak, A., Mills, A., Javitt, D.C., Schroeder, C.E., 2009. The leading sense: supramodal control of neurophysiological context by attention. Neuron 64, 419–430.
Lange, J., Oostenveld, R., Fries, P., 2011. Perception of the touch-induced visual double-flash illusion correlates with changes of rhythmic neuronal activity in human visual and somatosensory areas. Neuroimage 54, 1395–1405.
Lange, J., Oostenveld, R., Fries, P., 2013. Reduced occipital alpha power indexes enhanced excitability rather than improved visual perception. J. Neurosci. 33, 3212–3220.
Lennert, T., Samiee, S., Baillet, S., 2021. Coupled oscillations enable rapid temporal recalibration to audiovisual asynchrony. Commun. Bio. 4, 1–12.
Lo Verde, L., Morrone, M.C., Lunghi, C., 2017. Early Cross-modal Plasticity in Adults. J. Cogn. Neurosci. 29, 520–529.
Lunghi, C., Berchicci, M., Morrone, M.C., Di Russo, F., 2015a. Short-term monocular deprivation alters early components of visual evoked potentials. J. Physiol. 593, 4361–4372.
Lunghi, C., Burr, D.C., Morrone, C., 2011. Brief periods of monocular deprivation disrupt ocular balance in human adult visual cortex. Curr. Biol. 21, 538–539.
Lunghi, C., Emir, U.E., Morrone, M.C., Bridge, H., 2015b. Short-Term monocular deprivation alters GABA in the adult human visual cortex. Curr. Biol. 25, 1496–1501.
Lunghi, C., Sale, A., 2015. A cycling lane for brain rewiring. Curr. Biol. 25, R1122–R1123.
Lunghi, C., Sframeli, A.T., Lepri, A., Lepri, M., Lisi, D., Sale, A., Morrone, M.C., 2019. A new counterintuitive training for adult amblyopia. Ann. Clin. Transl. Neurol. 6, 274–284.
Macmillan, N.A., Creelman, C.D., 2004. Detection theory: A user's Guide. Psychology press.
Maris, E., Oostenveld, R., 2007. Nonparametric statistical testing of EEG-and MEG-data. J. Neurosci. Methods. 164, 177–190.
Merabet, L.B., Hamilton, R., Schlaug, G., Swisher, J.D., Kiriakopoulos, E.T., Pitskel, N.B., Kauffman, T., Pascual-Leone, A., 2008. Rapid and reversible recruitment of early visual cortex for touch. PLoS One 3, e3046.
Mishra, J., Martinez, A., Sejnowski, T.J., Hillyard, S.A., 2007. Early cross-modal interactions in auditory and visual cortex underlie a sound-induced visual illusion. J. Neurosci. 27, 4120–4131.
Moro, S.S., Steeves, J.K.E., 2018a. Normal temporal binding window but no sound-induced flash illusion in people with one eye. Exp. Brain Res. 236, 1825–1834.
Moro, S.S., Steeves, J.K.E., 2018b. Audiovisual plasticity following early abnormal visual experience: reduced McGurk effect in people with one eye. Neurosci. Lett. 672, 103–107.
Narinesingh, C., Goltz, H.C., Raashid, R.A., Wong, A.M.F., 2015. Developmental trajectory of McGurk effect susceptibility in children and adults with amblyopia. Invest. Ophthalmol. Vis. Sci. 56, 2107–2113.
Narinesingh, C., Goltz, H.C., Wong, A.M.F., 2017. Temporal binding window of the sound-induced flash illusion in amblyopia. Investig. Ophthalmol. Vis. Sci. 58, 1442–1448.
Oostenveld, R., Fries, P., Maris, E., Schoffelen, J.M., 2011. FieldTrip: open source software for advanced analysis of MEG, EEG, and invasive electrophysiological data. Comput. Intell. Neurosci. 2011.
Opoku-Baah, C., Wallace, M.T., 2020. Brief period of monocular deprivation drives changes in audiovisual temporal perception. J. Vis. 20, 1–13.
Pérez-Bellido, A., Ernst, M.O., Soto-Faraco, S., López-Moliner, J., 2015. Visual limitations shape audio-visual integration. J. Vis. 15, 1–15.
Polley, D.B., Steinberg, E.E., Merzenich, M.M., 2006. Perceptual learning directs auditory cortical map reorganization through top-down influences. J. Neurosci. 26, 4970–4982.
Pfurtscheller, G., Da Silva, F.L., 1999. Event-related EEG/MEG synchronization and desynchronization: basic principles. Clin. Neurophysiol. 110, 1842–1857.
Richards, M.D., Goltz, H.C., Wong, A.M.F., 2017. Alterations in audiovisual simultaneity perception in amblyopia. PLoS One 12, 1–20.
Rohe, T., Ehlis, A.C., Noppeney, U., 2019. The neural dynamics of hierarchical Bayesian causal inference in multisensory perception. Nat. Commun. 10, 1–17.
Schwenk, J.C.B., VanRullen, R., Bremmer, F., 2020. Dynamics of visual perceptual echoes following short-term visual deprivation. Cereb. Cortex Commun. 1, 1–11.
Shams, L., Kamitani, Y., Shimojo, S., 2000. What You See Is What You Hear. Nature 408, 2000.
Siegel, M., Donner, T.H., Engel, A.K., 2012. Spectral fingerprints of large-scale neuronal interactions. Nat. Rev. Neurosci. 13, 121–134.
Spolidoro, M., Sale, A., Berardi, N., Maffei, L., 2009. Plasticity in the adult brain: lessons from the visual system. Exp. Brain Res. 192, 335–341.
Stropahl, M., Bauer, A.K.R., Debener, S., Bleichner, M.G., 2018. Source-modeling auditory processes of EEG data using EEGLAB and brainstorm. Front. Neurosci. 12, 1–11.
Tadel, F., Baillet, S., Mosher, J.C., Pantazis, D., Leahy, R.M., 2011. Brainstorm: a user-friendly application for MEG/EEG analysis. Comput. Intell. Neurosci. 2011.
Tallon-Baudry, C., Bertrand, O., 1999. Oscillatory gamma activity in humans and its role in object representation. Trend. Cogn. Sci. 3, 151–162.
Turrigiano, G., 2012. Homeostatic synaptic plasticity: local and global mechanisms for stabilizing neuronal function. Cold Spring Harb. Perspect. Biol. 4.
Turrigiano, G.G., Nelson, S.B., 2004. Homeostatic plasticity in the developing nervous system. Nat. Rev. Neurosci. 5, 97–107.
Van Atteveldt, N., Murray, M.M., Thut, G., Schroeder, C.E., 2014. Multisensory integration: flexible use of general operations. Neuron 81, 1240–1253.
Vanes, L.D., White, T.P., Wigton, R.L., Joyce, D., Collier, T., Shergill, S.S., 2016. Reduced susceptibility to the sound-induced flash fusion illusion in schizophrenia. Psychiatry Res. 245, 58–65.
VanRullen, R., 2016. Perceptual cycles. Trend. Cogn. Sci. 20, 723–735.
Viola, F.C., Thorne, J., Edmonds, B., Schneider, T., Eichele, T., Debener, S., 2009. Semi-automatic identification of independent components representing EEG artifact. Clin. Neurophysiol. 120, 868–877.
Wang, M., McGraw, P., Ledgeway, T., 2020. Short-term monocular deprivation reduces inter-ocular suppression of the deprived eye. Vision Res. 173, 29–40.

Watkins, S., Shams, L., Tanaka, S., Haynes, J.D., Rees, G., 2006. Sound alters activity in human V1 in association with illusory visual perception. Neuroimage 31, 1247–1256.
Whittingham, K.M., McDonald, J.S., Clifford, C.W.G., 2014. Synesthetes show normal sound-induced flash fission and fusion illusions. Vision Res. 105, 1–9.
Yusuf, P.A., Hubka, P., Tillein, J., Kral, A., 2017. Induced cortical responses require developmental sensory experience. Brain 140, 3153–3165.
Zhou, J., Baker, D.H., Simard, M., Saint-Amour, D., Hess, R.F., 2015. Short-term monocular patching boosts the patched eye's response in visual cortex. Restor. Neurol. Neurosci. 33, 381–387.
Zhou, J., Clavagnier, S., Hess, R.F., 2013. Short-term monocular deprivation strengthens the patched eye's contribution to binocular combination. J. Vis. 13, 12.